

The Plasma Membrane H⁺-ATPase AHA1 Plays a Major Role in Stomatal Opening in Response to Blue Light¹

Shota Yamauchi, Atsushi Takemiya, Tomoaki Sakamoto², Tetsuya Kurata³, Toshifumi Tsutsumi, Toshinori Kinoshita, and Ken-ichiro Shimazaki*

Department of Biology, Faculty of Science, Kyushu University, Fukuoka 819-0395, Japan (S.Y., A.T., T.T., K.S.); Plant Global Education Project, Graduate School of Biological Sciences, Nara Institute of Science and Technology, Ikoma, Nara 630-0192, Japan (T.S., Te.K.); and Institute of Transformative Bio-Molecules (WPI-ITbM), Nagoya University, Chikusa, Nagoya 464-8602, Japan (To.K.)

ORCID IDs: 0000-0001-7621-1259 (T.K.); 0000-0001-6450-8506 (K.-i.S.).

Stomata open in response to a beam of weak blue light under strong red light illumination. A blue light signal is perceived by phototropins and transmitted to the plasma membrane H⁺-ATPase that drives stomatal opening. To identify the components in this pathway, we screened for mutants impaired in blue light-dependent stomatal opening. We analyzed one such mutant, provisionally named *blus2* (*blue light signaling2*), and found that stomatal opening in leaves was impaired by 65%, although the magnitude of red light-induced opening was not affected. Blue light-dependent stomatal opening in the epidermis and H⁺ pumping in guard cell protoplasts were inhibited by 70% in *blus2*. Whole-genome resequencing identified a mutation in the *AHA1* gene of the mutant at Gly-602. T-DNA insertion mutants of *AHA1* exhibited a similar phenotype to *blus2*; this phenotype was complemented by the *AHA1* gene. We renamed *blus2* as *aha1-10*. T-DNA insertion mutants of *AHA2* and *AHA5* did not show any impairment in stomatal response, although the transcript levels of *AHA2* and *AHA5* were higher than those of *AHA1* in wild-type guard cells. Stomata in *ost2*, a constitutively active *AHA1* mutant, did not respond to blue light. A decreased amount of H⁺-ATPase in *aha1-10* accounted for the reduced stomatal blue light responses and the decrease was likely caused by proteolysis of misfolded *AHA1*. From these results, we conclude that *AHA1* plays a major role in blue light-dependent stomatal opening in Arabidopsis and that the mutation made the *AHA1* protein unstable in guard cells.

Stomata regulate gas exchange between plants and the atmosphere and allow CO₂ provision for photosynthesis and transpiration. These latter processes facilitate the transport of minerals to plant tissues through the xylem system, resulting in plant growth under ever-changing

environments (Hetherington and Woodward, 2003; Roelfsema and Hedrich, 2005; Vavasseur and Raghavendra, 2005; Shimazaki et al., 2007). Stomatal aperture is finely regulated by light, water status, the phytohormone abscisic acid, and other environmental factors (Pandey et al., 2007; Kim et al., 2010). Blue light (390–550 nm) is one of the most effective stimuli for stomatal opening; blue light responses of stomata are almost ubiquitous in land plants from lycophytes to euphyllophytes, but not in *Polypodiopsida* (Doi et al., 2006, 2015). Some plant species require blue light for both stomatal opening and photosynthetic CO₂ fixation (Doi et al., 2015). Blue light is perceived by phototropins (*phot1* and *phot2*), which are plant-specific light-activated protein kinases associated with the plasma membrane (Kinoshita et al., 2001; Briggs and Christie, 2002). Phototropins contain two domains called LOV1 (light, oxygen, or voltage) and LOV2 close to the N terminus as photoreaction sites and a C-terminal Ser/Thr kinase (Christie, 2007; Tokutomi et al., 2008; Inoue et al., 2011). Illumination of plants with blue light results in the activation of phototropins by autophosphorylation and induces various responses, including phototropism, chloroplast movements, leaf flattening, and stomatal opening

¹ This work was supported by JSPS KAKENHI grant no. 26251032 (to K.S.) and 26711019 and 15K14552 (to A.T.), MEXT KAKENHI grant no. 25120719 (to A.T.), and Grants-in-Aid for Scientific Research for Plant Graduate Student from the Nara Institute of Science and Technology supported by the Ministry of Education, Culture, Sports, Science, and Technology of Japan

² Present address: Faculty of Life Sciences, Kyoto Sangyo University, Motoyama, Kamigamo, Kita-Ku, Kyoto 603-8555, Japan.

³ Present address: Graduate School of Life Sciences, Tohoku University, Aoba, Sendai 980-8578, Japan.

* Address correspondence to kenrcb@kyushu-u.org.

The author responsible for distribution of materials integral to the findings presented in this article in accordance with the policy described in the Instructions for Authors (www.plantphysiol.org) is: Ken-ichiro Shimazaki (kenrcb@kyushu-u.org).

S.Y., A.T., and K.S. conceived and designed the experiments; S.Y. performed most of the experiments; T.S. and Te.K. performed the next-generation sequencing and data analysis; T.T. carried out mutant screening; S.Y., A.T., Te.K., To.K., and K.S. analyzed data and wrote the manuscript.

www.plantphysiol.org/cgi/doi/10.1104/pp.16.01581

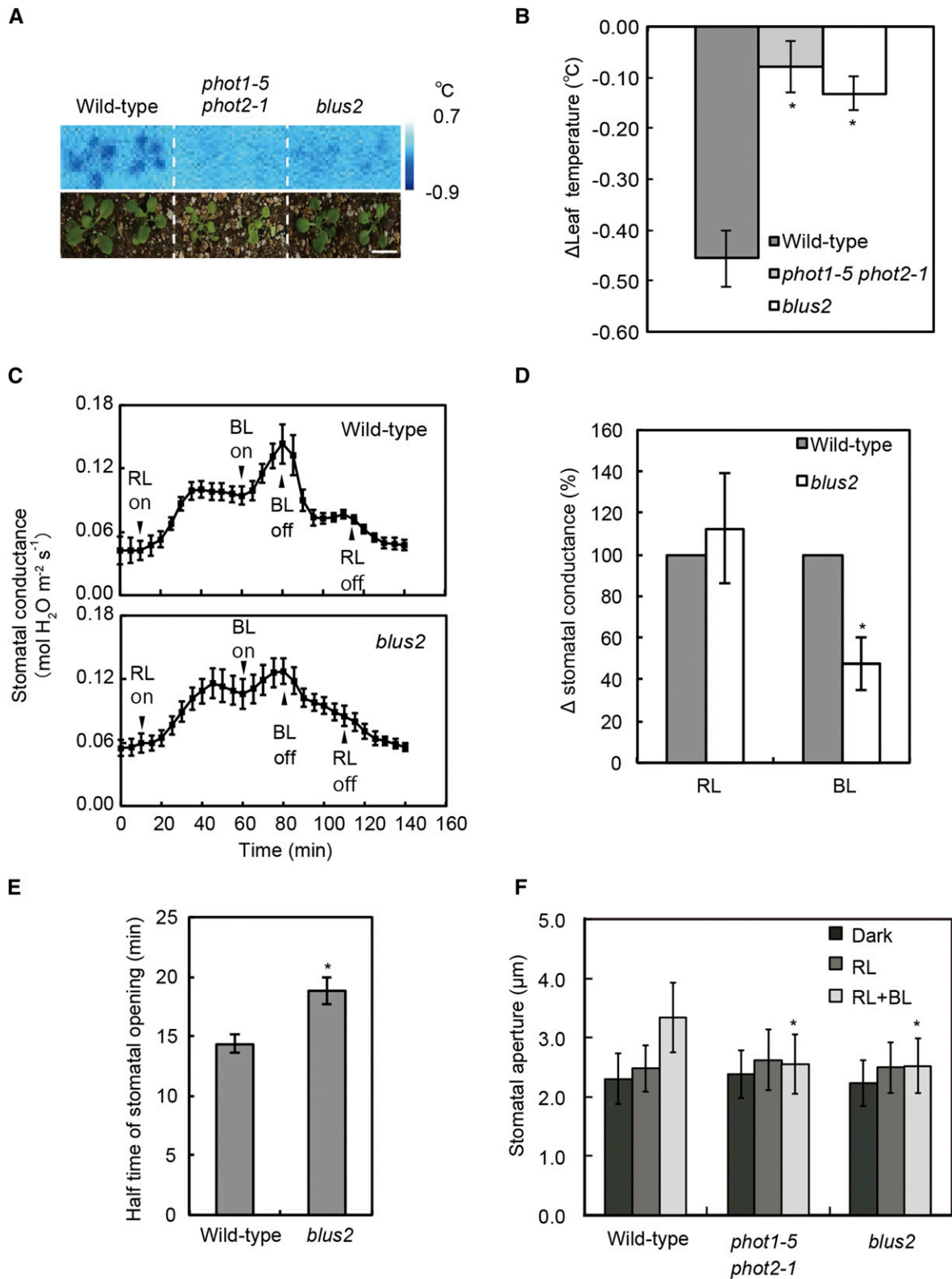


Figure 1. Impaired response of stomata to blue light in the *blus2* mutant. **A**, Thermal images of blue light responses of Arabidopsis wild-type, *phot1-5 phot2-1*, and *blus2* mutants. Plants were illuminated with red light ($80 \mu\text{mol m}^{-2} \text{s}^{-1}$) for 50 min, followed by blue light ($5 \mu\text{mol m}^{-2} \text{s}^{-1}$) for 15 min. The leaf temperature image was visualized by subtraction of thermal images created before and after 15 min illumination of blue light. Bar = 1 cm. **B**, Quantification of leaf temperature decrease in response to blue light.

(Inoue et al., 2008, 2010). In guard cells, signals from activated phototropins are transmitted to the plasma membrane H⁺-ATPases and induce phosphorylation-dependent activation and subsequent binding of 14-3-3 proteins (Kinoshita and Shimazaki, 1999; Svennelid et al., 1999). The activated H⁺-ATPases drive K⁺ uptake through the hyperpolarization-activated inwardly rectifying K⁺ (K_{in}⁺) channels in the plasma membranes, and the resulting K⁺-salt accumulation in guard cells elicits stomatal opening (Assmann, 1993; Roelfsema and Hedrich, 2005; Shimazaki et al., 2007; Kim et al., 2010). The signals from activated phototropins are likely transmitted to SLAC1-type anion channels for inhibition (Marten et al., 2007; Negi et al., 2008; Vahisalu et al., 2008) and K_{in}⁺ channels for activation (Zhao et al., 2012), both of which facilitate stomatal opening, although the exact nature of the events is not understood. A protein phosphatase 1 and its regulator PRSL1 mediate the signaling between phototropins and the H⁺-ATPase (Takemiya et al., 2006, 2013a), and an unidentified protein kinase(s) may catalyze the phosphorylation of H⁺-ATPase for its activation.

Previously, we developed a screening strategy using infrared thermography to isolate *Arabidopsis* (*Arabidopsis thaliana*) mutants impaired in stomatal opening specific to blue light (Takemiya et al., 2013b). Using this screen, we obtained several mutants and demonstrated that a novel Ser/Thr protein kinase BLUS1 undergoes phosphorylation as a phototropin substrate and functions as an initial step in phototropin signaling in response to blue light. However, the signaling mechanisms by which phototropins transduce the light signal into downstream responses are not fully understood.

The plasma membrane H⁺-ATPase acts as a primary transporter in fungi and plants, and drives a large number of secondary transporters by enhancing the membrane potential and pH gradient across the plasma membrane (Palmgren, 2001). The H⁺-ATPase is activated in response to various signals such as blue light, osmotic shock, Suc, and the phytohormone auxin (Kinoshita and Shimazaki, 1999; Kerkeb et al., 2002; Niittylä et al., 2007; Takahashi et al., 2012; Okumura et al., 2016). There are 11 isoforms of H⁺-ATPase in *Arabidopsis*. Several isoforms have been shown to exhibit organ and development specific functions in *Arabidopsis*, such as salt tolerance (AHA4; Vitart et al., 2001), seed coat endothelium (AHA10; Baxter et al.,

2005), pollen development (AHA3; Robertson et al., 2004), and embryo formation (AHA1 and AHA2; Haruta et al., 2010). However, functional specificity of H⁺-ATPase isoforms has not been reported for *Arabidopsis* stomatal guard cells. The isoforms are thought to function redundantly in stomatal opening, and the 11 isoforms are all expressed in guard cells with high expression levels for AHA1, AHA2, and AHA5 (Ueno et al., 2005). The isoforms AHA1, AHA2, AHA3, and AHA5 belong to the same H⁺-ATPase subfamily in *Arabidopsis* (Arango et al., 2003). By contrast, constitutive activation of AHA1 keeps stomata open (Merlot et al., 2007), and overexpression of AHA2 in guard cells promotes light-induced stomatal opening that results in the enhancement of plant growth (Wang et al., 2014), suggesting the functional importance of specific isoforms in guard cells. In mesophyll cells, only four isoforms are expressed (Ueno et al., 2005).

In this study, we performed genome resequencing of a mutant that was demonstrated by thermography to be impaired in blue light-dependent stomatal opening and found that AHA1 was the responsible gene. We also showed that AHA1 has a major role in stomatal opening in response to blue light, while other AHA genes that are highly expressed in guard cells, such as AHA2 and AHA5, do not play an essential role in this response.

RESULTS

Blue Light Response of Stomata Is Impaired in the *blus2* Mutant

We used infrared thermography to screen an M2 population from ethyl methanesulfonate-mutagenized *Arabidopsis* (*Col-g11*) for mutants that showed impaired stomatal opening specific to blue light. We identified a mutant that showed only a small leaf temperature decrease in response to blue light under moderate red light (80 $\mu\text{mol m}^{-2} \text{s}^{-1}$; Fig. 1, A and B). Wild-type control plants showed a clear temperature decrease, while the double mutant *phot1-5 phot2-1*, which is unresponsive to blue light, did not show a temperature decrease. Stomatal conductance in wild-type plants increased under strong red light (600 $\mu\text{mol m}^{-2} \text{s}^{-1}$) to reach a steady state; it was further increased by weak blue light (20 $\mu\text{mol m}^{-2} \text{s}^{-1}$) superimposed on the red light (Fig. 1C). In the mutant, stomatal conductance was increased by the red light to

Figure 1. (Continued.)

Leaf temperature was quantified using PE Professional software (NEC Avio Infrared Technologies). Bars represent $\pm \text{SE}$ ($n = 5$; $*P < 0.01$). C, Light-dependent stomatal opening, as measured by stomatal conductance, in intact leaves of wild-type *Arabidopsis* and *blus2*. Red light (600 $\mu\text{mol m}^{-2} \text{s}^{-1}$) and blue light (20 $\mu\text{mol m}^{-2} \text{s}^{-1}$) were switched on/off as indicated. Bars represent $\pm \text{SE}$ ($n = 4$). D, Absolute increase of stomatal conductance in response to red light and blue light. Bar represents $\pm \text{SE}$ ($n = 4$; $*P < 0.05$). E, Half-time of stomatal opening in response to red light of the wild type and *blus2*. We obtained the maximum stomatal conductance and the time required for reaching this point after red light illumination and the conductance just before the illumination. We drew an approximate straight line using these parameters and calculated half-time required to reach the maximum conductance in the wild type and *blus2*. Bar represents $\pm \text{SE}$ ($n = 4$; $*P < 0.05$). F, Light-dependent stomatal opening in epidermal peels from wild-type *Arabidopsis* and mutants. Epidermis peels from dark-adapted plants were illuminated by red light (60 $\mu\text{mol m}^{-2} \text{s}^{-1}$) or red light (50 $\mu\text{mol m}^{-2} \text{s}^{-1}$) and blue light (10 $\mu\text{mol m}^{-2} \text{s}^{-1}$) for 2 h. Bars represent $\pm \text{SD}$ ($n = 75$ stomata; $*P < 0.01$).

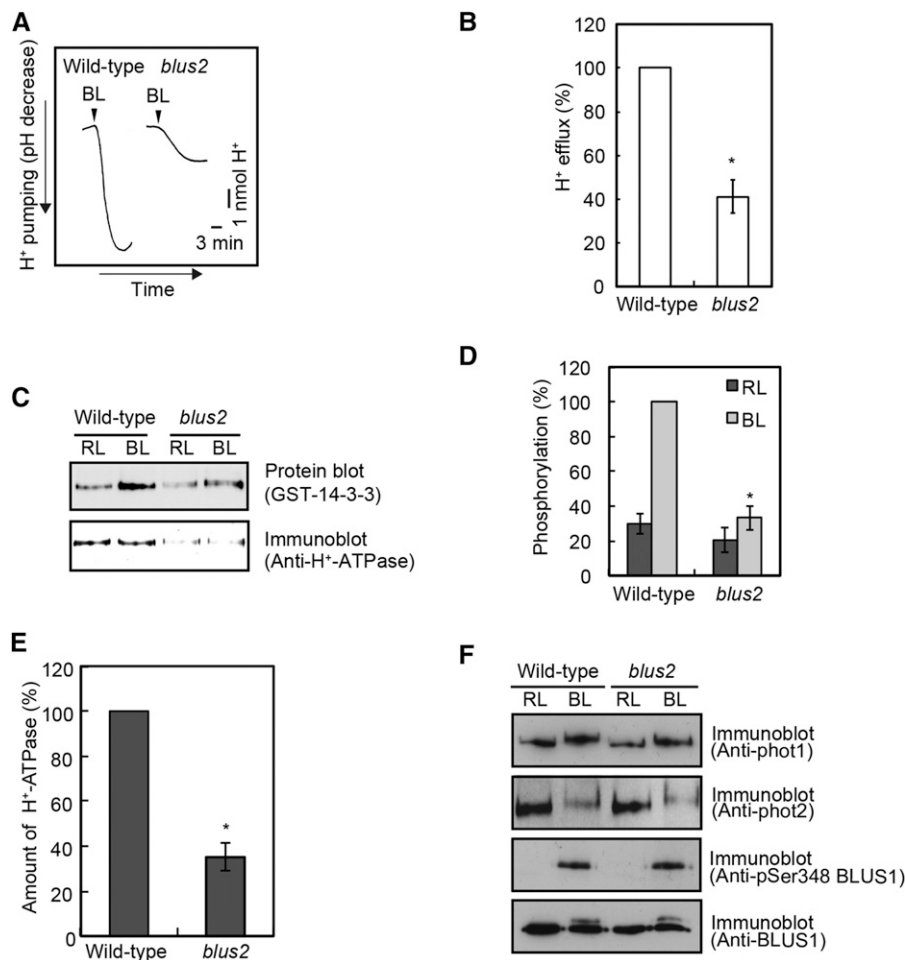


Figure 2. Decrease of H⁺-ATPase in guard cell of *blus2* mutant. A, Blue light-dependent H⁺ pumping of guard cell protoplasts from the wild type and *blus2*. Protoplasts were incubated with red light ($600 \mu\text{mol m}^{-2} \text{s}^{-1}$) illumination for 2 h, and a pulse of blue light ($100 \mu\text{mol m}^{-2} \text{s}^{-1}$; 30 s) was applied as indicated ($n = 3$). B, Relative quantification of maximum rate of H⁺ pumping and H⁺ efflux from guard cell protoplasts ($n = 3$ independent experiments; $*P < 0.01$). C, Phosphorylation of H⁺-ATPase in response to blue light. Guard cell protoplasts were incubated under red light ($600 \mu\text{mol m}^{-2} \text{s}^{-1}$) for 30 min, then a pulse of blue light ($100 \mu\text{mol m}^{-2} \text{s}^{-1}$; 30 s) was applied for 3 min. Phosphorylation was quantified by protein blot using 14-3-3 protein. Upper panel shows H⁺-ATPase phosphorylation. Lower panel shows immunoblot using H⁺-ATPase-specific antibodies. Each lane contains 2.5 μg (protein blot) or 5 μg (immunoblot) of protein ($n = 9$; $*P < 0.01$). D, Relative phosphorylation in response to blue light. Phosphorylation was quantified using ImageJ. Bars represent $\pm \text{SE}$ ($n = 9$; $*P < 0.01$). E, Relative quantification of H⁺-ATPase in guard cell protoplasts. The H⁺-ATPase was reacted with specific antibodies and the band images were quantified using ImageJ. Bars represent $\pm \text{SE}$ ($n = 9$ independent experiments; $*P < 0.01$). F, Phosphorylation of phototropins and BLUS1. Guard cell protoplasts were incubated as described in A. Reaction was terminated after 2 min of blue light illumination. Immunodetection was performed using phot1, phot2, BLUS1, and BLUS1 pSer 348 antibodies. Each lane contains 8 μg of proteins ($n = 3$).

the same magnitude as in wild-type plants, but the rate of conductance increase was slightly lower (Fig. 1, C–E). The half-time required for the maximum magnitude was 14 min for wild-type plants and 18 min for the mutant in response to red light. The blue light response was inhibited by about 60% in both rate and magnitude (Fig. 1, C and D). In epidermal peels, the red light-induced opening response was very small in both wild-type and mutant plants, and stomatal opening by blue light was almost completely inhibited in the mutant (Fig. 1F). No difference was found in stomatal aperture among the plants under dark conditions. These results suggest that blue light-dependent stomatal

opening is impaired in the mutant. We provisionally named the mutant *blus2* (*blue light signaling2*).

Amount of the Plasma Membrane H⁺-ATPase Is Decreased in Guard Cells of *blus2*

Since stomatal opening in response to blue light is driven by H⁺ pumping in guard cells, we examined H⁺ pumping in guard cell protoplasts from *blus2* and found that it was inhibited by 70% (Fig. 2, A and B). We indirectly determined the phosphorylation status of the plasma membrane H⁺-ATPase by a 14-3-3 protein

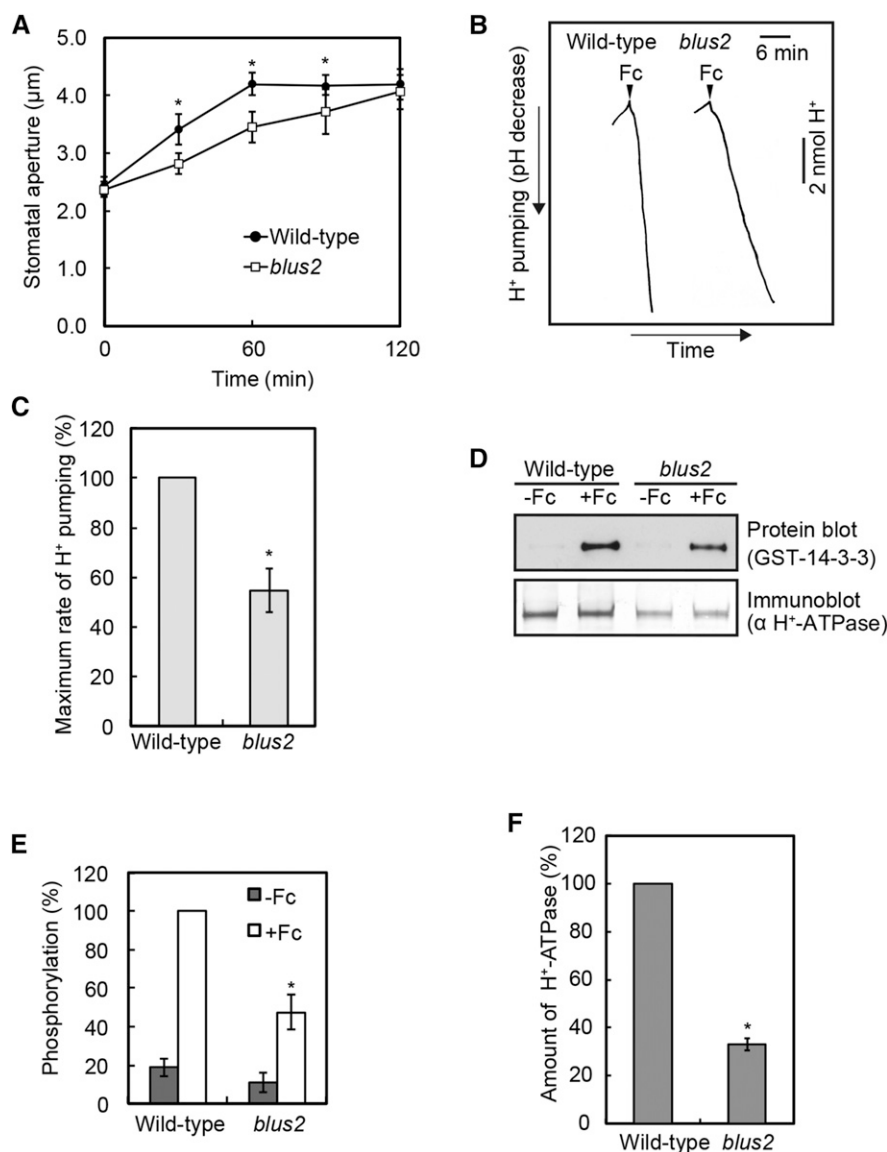


Figure 3. Impaired fusicoccin (Fc) response in *blus2* mutant. **A**, Fc-dependent stomatal opening in epidermal peels. Epidermal peels from dark-adapted plants were incubated with Fc (final concentration 10 μM). Stomatal aperture was measured after 0, 30, 60, 90, and 120 min after Fc application. Bars represent $\pm\text{SD}$ ($n = 5$ independent experiments; $*P < 0.05$). **B**, Fc-dependent H^+ pumping of guard cell protoplasts. Guard cell protoplasts were incubated with red light illumination (600 $\mu\text{mol m}^{-2} \text{s}^{-1}$) for 2 h; 10 μM Fc was applied as indicated ($n = 3$). **C**, Relative quantification of maximum rate of H^+ pumping from guard cell protoplasts ($n = 3$; $*P < 0.01$). **D**, Fc-dependent H^+ -ATPase phosphorylation in guard cell. Guard cell protoplasts were incubated for 30 min with red light illumination (600 $\mu\text{mol m}^{-2} \text{s}^{-1}$). A final concentration of 10 μM Fc was applied to the reaction mixture. Reaction was terminated after 3 min from Fc application. Upper panel shows Fc-dependent H^+ -ATPase phosphorylation. Lower panel shows immunoblot using H^+ -ATPase antibodies. Each lane contains 2.5 μg (protein blot) or 5 μg (immunoblot) of proteins ($n = 9$). **E**, Relative phosphorylation in response to Fc. Phosphorylation was quantified using ImageJ. Bars represent $\pm\text{SE}$ ($n = 9$; $*P < 0.05$). **F**, Relative quantification of H^+ -ATPase in guard cell protoplasts. Amount was quantified using ImageJ. Bars represent $\pm\text{SE}$ ($n = 9$ independent experiments; $*P < 0.01$).

binding to the H^+ -ATPase in guard cell protoplasts. The H^+ -ATPase in wild-type plants was phosphorylated in response to blue light, while it was only 30% phosphorylated in the mutant (Fig. 2, C and D). Interestingly, the amount of H^+ -ATPase was reduced to 35% in the mutant (Fig. 2E). Next, we performed immunological analysis to determine whether other components in this signaling pathway in guard cells, such as phototropins (phot1 and phot2) and BLUS1 kinase, were affected. The analysis indicated that the amounts of phot1 and phot2 were not altered and that phot1 and phot2 were normally phosphorylated in the *blus2* mutant (Fig. 2F). The amount of BLUS1 was not reduced and it was phosphorylated at the physiological site Ser-348, in agreement with previous work (Takemiya et al., 2013b; Fig. 2F). The results indicate that the impairment of stomatal opening in response to blue light was due to a reduction in the amount of H^+ -ATPase in guard cells.

Stomatal Opening by Fusicoccin Is Impaired in the *blus2* Mutant

As reduction in the amount of H^+ -ATPase in guard cells appeared to be responsible for the impairment of stomatal responses, we postulated that fusicoccin-induced stomatal opening might also be suppressed because fusicoccin directly activates H^+ -ATPase. As shown in Figure 3A, the rate of stomatal opening after fusicoccin treatment was reduced in the mutant compared to wild-type plants. The rate of H^+ pumping in guard cell protoplasts by fusicoccin was decreased to 50% (Fig. 3, B and C), with an accompanying decrease in phosphorylation levels of H^+ -ATPase in the *blus2* mutant (Fig. 3, D and E). However, the reductions in rate of H^+ pumping and level of phosphorylation were less in the fusicoccin-induced responses compared to blue light responses in the *blus2* mutant. This difference is probably due to the reversible dephosphorylation of

Table I. Identification of the gene responsible for *blus2* by next-generation sequencing

Total reads from <i>blus2</i> genome by GAllx and percentage of reads aligned to reference wild-type genome.		
<i>blus2</i>	Numbers of Reads	Percentage of Aligned Reads
Aligned to reference	35,568,396	85.98
Unaligned to reference	5,800,492	14.02
Unknown reads	0	0

the H⁺-ATPase that deactivates H⁺ pumping activity; dephosphorylation proceeds in blue light-dependent responses, but the reactions are arrested in fusicocin-induced events. The amount of H⁺-ATPase was not changed by fusicocin treatment (Fig. 3F).

AHA1 Gene Is Mutated in *blus2*

To identify the gene responsible for the *blus2* phenotype, we performed whole-genome resequencing using F2 plants of a backcross population. An 86% read was aligned to the wild-type genome sequence (Table I). We focused on four candidate genes (Table II) and identified a base pair change in H⁺-ATPase isoform *AHA1* (*Arabidopsis* H⁺-ATPase1). The *AHA1* gene of *At2g18960* in *blus2* mutant has a G-to-A point mutation at nucleotide 3705, which results in a Gly-to-Asp amino acid substitution at position 602 (Fig. 4A). We transformed the *blus2* mutant with *AHA1* and infrared thermographic analysis showed complementation of the stomatal phenotype (Fig. 4, B and C). The results indicate that the impairment of stomatal opening by blue light is due to a lesion of the *AHA1* gene, which resulted in a reduction in the production of H⁺-ATPase.

We obtained the SAIL_1285_D12 mutant line in which T-DNA was inserted in the third exon of *AHA1* (*aha1-9*; Fig. 4A). RT-PCR analysis of *AHA1* expression revealed that the mutant is a null allele (Supplemental Fig. S1). The *aha1-9* mutant exhibited impairment in blue light-dependent stomatal opening in both intact leaves (Fig. 4, D–F) and the epidermis (Fig. 4G) and showed essentially the same phenotype as the *blus2* mutant (Fig. 1). The *aha1-9* mutant showed similar phenotypes as the *blus2* mutant in H⁺ pumping and phosphorylation of the H⁺-ATPase in response to blue light and fusicocin (Supplemental Fig. S2, A–C). The amount of H⁺-ATPase in *aha1-9* was reduced to 35%, similar to the reduction in *blus2* (Supplemental Fig. S2D). Furthermore, the rate of red light-induced stomatal opening was decreased in

aha1-9 as in *blus2*; the half-times for maximum magnitude were 13 min for the wild type and 17 min for *aha1-9*. The results indicate that impairment of stomatal opening in *blus2* is brought about by the mutation of the *AHA1* gene.

F1 backcrosses showed that *blus2* and *aha1-9* mutations are recessive alleles (Supplemental Fig. S3A). Crosses between single *blus2* and *aha1-9* mutants revealed the same impairment in leaf temperature change in response to blue light as the single mutants (Supplemental Fig. S3B), confirming that *AHA1* is the gene responsible gene for the *blus2* phenotype. We therefore renamed *blus2* as *aha1-10*.

Stomatal Blue Light Response in the *ost2* Mutant

Merlot et al. (2007) identified the constitutively active *AHA1* mutants *ost2-1D* and *ost2-2D*. We therefore expected that stomata in the constitutive active *AHA1* mutants hardly respond to blue light. In the mutant screen performed here, we identified a mutant whose stomata opened in the dark and found that this mutation affected amino acid residue P68S, just as in *ost2-1D*. Since the *ost2-1D* mutant is derived from the *Ler* background, we named our mutant as *ost2-3D*. Wild-type and *phot1-5 phot2-1* double mutant plants showed leaf temperatures of 21°C, whereas *ost2-3D* had a temperature of 18.5°C due to wide stomatal opening in the dark (Fig. 5A, upper panel). These three plant types were then illuminated with red light at 80 μmol m⁻² s⁻¹ for 50 min and exposed to weak blue light at 5 μmol m⁻² s⁻¹ for 15 min. Subtraction images before and after blue light application (Fig. 5B, lower panel) revealed that leaf temperatures decreased by 0.25°C in wild-type plants, but not in the *phot1-5 phot2-1. ost2-3D* mutants exhibited only a slight leaf temperature decrease in response to blue light (Fig. 5C). Epidermal peels of *ost2-3D* showed that stomata opened widely in the dark and that no further actual opening occurred in response to blue light (Fig. 5D). The results further support our conclusion

Table II. Candidate genes of *blus2*

Reference	Variant Allele	Gene	Gene Symbol	Exon Number	Position in Protein	Amino Acid Change
G	A	AT2G18240	AT2G18240	2	191	S→N
G	A	AT2G18960	AHA1	9	602	G→D
G	A	AT2G36790	UGT73C6	1	252	P→L
G	A	AT2G38823	AT2G38823	2	70	A→T

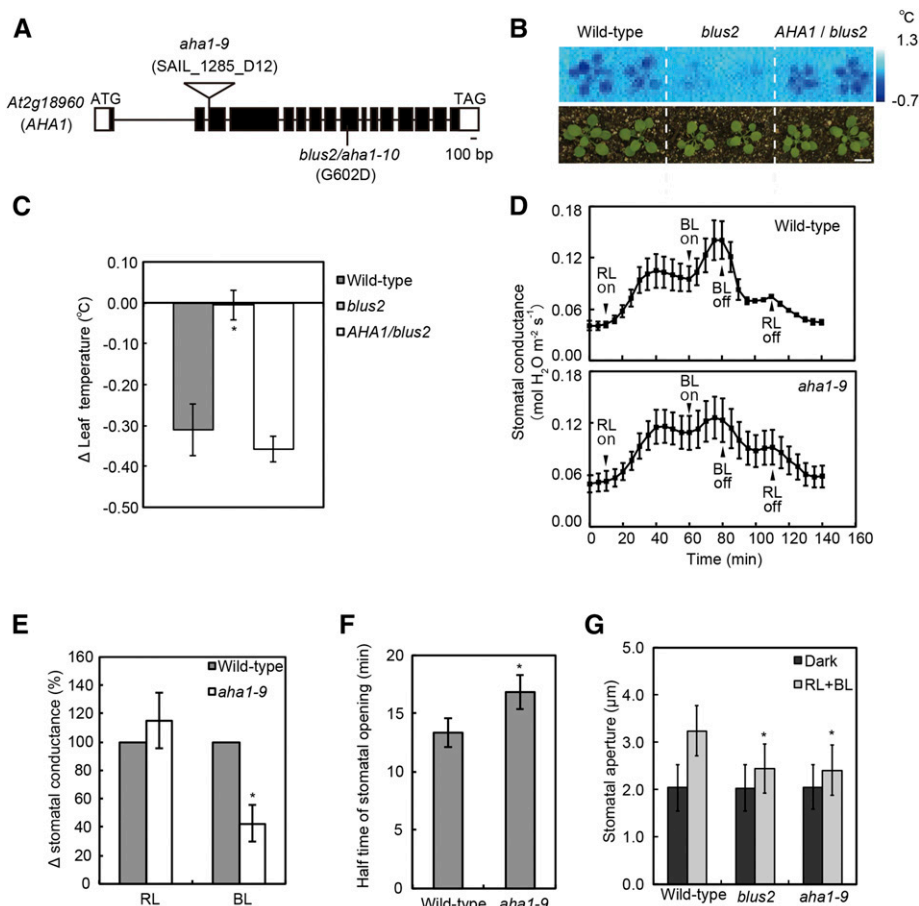


Figure 4. Impaired H⁺-ATPase isoform, AHA1 affects blue light-dependent stomatal opening. **A**, Structure of *At2g18960* gene, which encodes AHA1. Black boxes indicate exons, and white boxes indicate untranslated region. Line indicates introns. Bar = 100 bp. **B**, Thermal images of the wild type, *blus2*, and *AHA1/blus2* transgenic line. Bar = 1 cm. Plants were illuminated with red light ($80 \mu\text{mol m}^{-2} \text{s}^{-1}$) for 50 min, followed by blue light ($5 \mu\text{mol m}^{-2} \text{s}^{-1}$) for 15 min. The leaf temperature image was visualized by subtraction of thermal images created before and after 15 min illumination of blue light. Bar = 1 cm. **C**, Quantification of leaf temperature decrease in response to blue light. Leaf temperature was quantified using PE Professional software (NEC Avio Infrared Technologies). Bars represent $\pm \text{SE}$ ($n = 8$; $*P < 0.01$). **D**, Light-dependent stomatal opening, as measured by stomatal conductance, in intact leaves of wild-type *Arabidopsis* and *aha1-9*. Red light ($600 \mu\text{mol m}^{-2} \text{s}^{-1}$) and blue light ($20 \mu\text{mol m}^{-2} \text{s}^{-1}$) were switched on/off as indicated. Bars represent $\pm \text{SE}$ ($n = 4$). **E**, Absolute increase of stomatal conductance in response to red light and blue light of the wild type and *aha1-9*. Bars represent $\pm \text{SE}$ ($n = 4$; $*P < 0.05$). **F**, Half-time of stomatal opening in response to red light. The half-times were determined as in Fig. 1E. Bar represents $\pm \text{SE}$ ($n = 4$; $*P < 0.05$). **G**, Light-dependent stomatal opening in epidermal peels from wild-type *Arabidopsis* and mutants. Epidermis peels from dark-adapted plants were illuminated by red light ($50 \mu\text{mol m}^{-2} \text{s}^{-1}$) and blue light ($10 \mu\text{mol m}^{-2} \text{s}^{-1}$) for 2 h. Bars represent $\pm \text{SD}$ ($n = 75$ stomata; $*P < 0.01$).

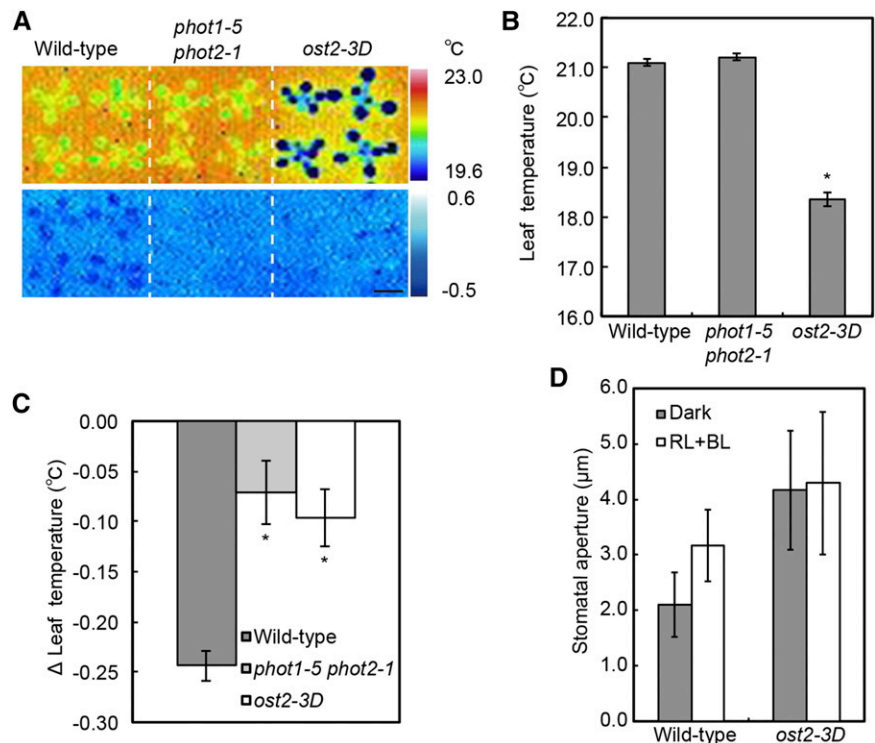
that AHA1 plays a major role in blue light-dependent stomatal opening in *Arabidopsis*.

Role of AHA2 and AHA5 in Blue Light-Dependent Stomatal Opening

Eleven H⁺-ATPase isoforms are expressed in *Arabidopsis* guard cells, with high expression of the *AHA1*, *AHA2*, and *AHA5* genes (Ueno et al., 2005); this suggests that some isoforms may function redundantly in the regulation of stomatal opening. To investigate the role of the AHA2 and AHA5 isoforms in the stomatal

response, we obtained a knockdown allele of *aha2-4* and a knockout allele of *aha5-2* (Supplemental Fig. S4, A and B). Infrared thermal images showed that the mutants of both *aha2-4* and *aha5-2* exhibited decreased leaf temperatures as observed in wild-type plants (Fig. 6A; Supplemental Fig. S4C). Likewise, *aha2-4* and *aha5-2* exhibited the typical blue light-dependent stomatal opening in epidermal peels (Fig. 6B) and both mutants showed normal blue light-dependent H⁺ pumping in guard cell protoplasts (Fig. 6, C and D). Immunological analysis showed that the amount of H⁺-ATPase was not reduced in either *aha2-4* or *aha5-2* (Fig. 6, E and F). Since the H⁺-ATPase antibodies used in this study were

Figure 5. *ost2* mutation affects blue light-dependent stomatal opening. A, Thermal images of dark conditions and blue light responses of Arabidopsis wild-type, *phot1-5 phot2-1*, and *ost2-3D* mutants. Upper panel: thermal image of dark conditions. Plants were kept overnight in the dark and leaf temperature was measured by infrared thermography. Lower panel: subtracted images of blue light responses. Plants were illuminated with red light ($80 \mu\text{mol m}^{-2} \text{s}^{-1}$) for 50 min, followed by blue light ($5 \mu\text{mol m}^{-2} \text{s}^{-1}$) for 15 min. The leaf temperature image was visualized by subtraction of thermal images created before and after 15 min illumination of blue light. Bar = 1 cm. B, Leaf temperature of the wild type, *phot1-5 phot2-1*, and *ost2-3D* in dark conditions. Bars represent $\pm \text{SE}$ ($n = 10$; $*P < 0.01$). C, Quantification of leaf temperature decrease in response to blue light. Bars represent $\pm \text{SE}$ ($n = 10$; $*P < 0.01$). D, Blue light-dependent stomatal opening in the epidermal peels of the wild type and *ost2-3D* mutant. Bars represent $\pm \text{SD}$ ($n = 75$ stomata).



raised against the catalytic domain of VHA2 (*Vicia faba* H⁺-ATPase2; Kinoshita and Shimazaki, 1999), it is possible that the antibodies exclusively recognized AHA1 and did not recognize AHA2 or AHA5. To eliminate this possibility, we produced recombinant GST fusions of the catalytic region of AHA1, AHA2, and AHA5 that corresponded to the VHA2 catalytic region. Immunoblot analysis showed that the antibodies utilized here recognized all these recombinant proteins (Supplemental Fig. S5), therefore excluding the potential problem raised above. Our results indicate that AHA1 is expressed at higher protein levels than AHA2 and AHA5 in guard cells and that AHA1 has a major function in blue light-dependent stomatal opening in Arabidopsis.

Expression of AHA1 Transcript in Guard Cells of Wild-Type and Mutant Plants

The immunological analysis of AHA isoforms described above indicated that the transcript levels of AHA1 were likely to be higher than those of AHA2 and AHA5 in guard cells. To confirm this, we used quantitative real-time PCR of cDNAs produced from total RNAs of guard cell protoplasts of wild-type and mutant plants (Supplemental Fig. S6). Unexpectedly, however, AHA1 expression was the lowest of the tested AHAs: AHA2 and AHA5 transcript levels were 1.7- and 3.5-fold higher than that of AHA1. This result suggests AHA1 is not the major isogene at the transcript level. We also determined the amount of AHA1 transcript in

guard cell protoplasts from *aha1-10* and found that this was comparable to the wild-type plants (Supplemental Fig. S7).

AHA1 Is Degraded in *aha1-10* in a Proteasome-Dependent Pathway

The *aha1-10* mutation caused a reduction in the amount of H⁺-ATPase to a level similar to that in *aha1-9*, an AHA1 null allele mutant (Fig. 2E; Supplemental Fig. S3D). Since the AHA1 transcript was not reduced in the *aha1-10* mutant (Supplemental Fig. S7), it is likely that misfolded AHA1 proteins were formed and then degraded in the mutant. Misfolded proteins are usually degraded by proteasome-dependent or -independent systems in the cytoplasm of eukaryotic cells (Schmitz and Herzog, 2004; Piper and Luzio, 2007). To examine whether degradation of misfolded AHA1 proteins occurred in *aha1-10*, we treated guard cell protoplasts with the proteasome inhibitor MG132. We found that the level of H⁺-ATPase increased in the mutant to the same level as in wild-type plants; wild-type plants showed no response in terms of H⁺-ATPase to MG132 (Fig. 7, A and B). The analysis suggests that misfolded AHA1 proteins were degraded in the ubiquitin-proteasome pathway. We next treated guard cell protoplasts with the protease inhibitors apronitin (10 μM), N^α-tosyl-lys chloromethyl ketone (TLCK; 1 mM), or a 1% cocktail of protease inhibitors. The level of H⁺-ATPase did not change significantly in wild-type plants, but the treatments did increase the level

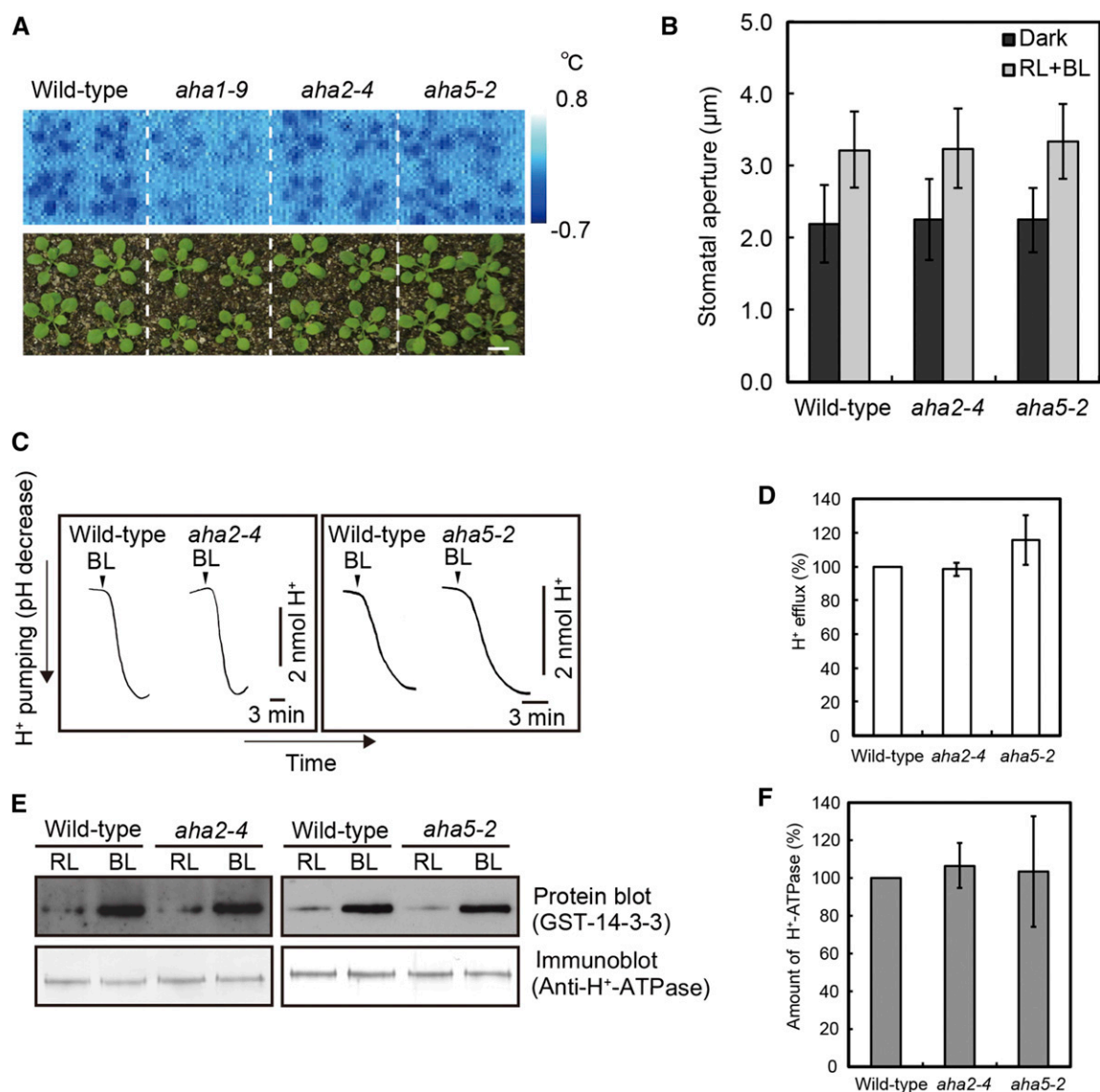


Figure 6. *aha2-4* and *aha5-2* mutants are not affected in blue light-dependent stomatal opening. A, Thermal images of the wild type, *aha1-9*, *aha2-4*, and *aha5-2* mutant responses to blue light. Plants were illuminated with red light ($80 \mu\text{mol m}^{-2} \text{s}^{-1}$) for 50 min, followed by blue light ($5 \mu\text{mol m}^{-2} \text{s}^{-1}$) for 15 min. The leaf temperature image was visualized by subtraction of thermal images created before and after 15 min illumination of blue light. Bar = 1 cm. B, Blue light-dependent stomatal opening in the epidermal peels of the wild type, *aha2-4*, and *aha5-2* mutants. Bars represent \pm SD ($n = 75$ stomata). C, Blue light-dependent H⁺ pumping in protoplasts of the wild type, *aha2-4*, and *aha5-2* mutants. Blue light illumination was applied as indicated ($n = 3$). D, Relative quantification of maximum rate of H⁺ pumping and H⁺ efflux from guard cell protoplasts ($n = 3$ independent experiments). E, Blue light-dependent phosphorylation of H⁺-ATPase in *aha2-4* and *aha5-2*. Upper panel shows H⁺-ATPase phosphorylation. Lower panel shows immunoblot using H⁺-ATPase specific antibodies. Each lane contains 2.5 μg (protein blot) or 5 μg (immunoblot) of proteins ($n = 3$). F, Relative quantification of H⁺-ATPase in guard cell protoplasts ($n = 3$ independent experiments).

in the *aha1-10* mutant up to that of the wild type (Supplemental Fig. S8, A and B). Since chymotrypsin-like proteins and/or trypsin-like proteins, which function in the proteasome, are sensitive to the protease inhibitors used. It is likely that protease inhibitors are also effective to prevent protein degradation in proteasome pathway (Lorenzo et al., 2002). Overall, we conclude that misfolded AHA1

proteins were formed and then degraded through the proteasome system.

DISCUSSION

The identification of a mutation in *AHA1* as responsible for the phenotype was a surprise as all 11 Arabidopsis H⁺-ATPase isoforms are expressed in guard cells

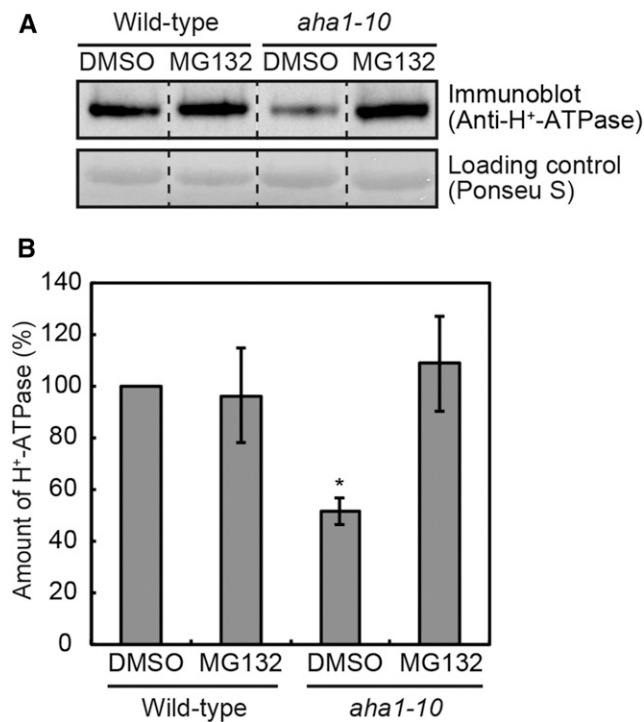


Figure 7. Effect of proteasome inhibitor on the amount of H⁺-ATPase in guard cell protoplasts. A, Immunoblot of H⁺-ATPase after treatment of guard cell protoplasts with MG132. Guard cell protoplasts from wild-type and *aha1-10* plants were incubated with 50 μ M MG132 for 30 min at 24°C. Upper panel shows immunoblot using the H⁺-ATPase antibodies. Lower panel shows Ponceau S staining as loading controls. Each lane contains 5 μ g proteins of guard cell protoplasts ($n = 3$). B, Quantification of the amount of H⁺-ATPase. Amount was quantified using ImageJ, and the relative values to the controls are expressed. Bars represent \pm SE ($n = 3$; * $P < 0.01$).

(Ueno et al., 2005), with high expression levels of *AHA2* and *AHA5*, and the isoforms are thought to function redundantly in stomatal opening. We tested the roles of *AHA2* and *AHA5* in stomatal responses and found that the blue light responses of stomata were not altered in *aha2* and *aha5* single mutants. These observations were in agreement with the conclusion that *AHA1* plays a major role in blue light-dependent stomatal opening (Fig. 6). The importance of *AHA1* or *AHA2* for stomatal opening has been demonstrated by induction of dominant mutations or overexpression of individual *AHA* genes in guard cells of Arabidopsis (Merlot et al., 2007; Wang et al., 2014). Analyses of loss-of-function *AHA1* genes with respect to stomatal opening together with those of *aha2* and *aha5* mutants provided genetic evidence for the important role of *AHA1* in blue light-dependent stomatal opening. We note here that the blue light response of stomata in the *aha1-10* mutant was not completely inhibited in intact leaves, with 30 to 40% of the responsiveness being retained. The remaining activities are probably driven by other isoforms of H⁺-ATPases in the guard cells.

Why does the *AHA1* isoform in guard cells play a major role for blue light-dependent stomatal opening in

Arabidopsis? One possibility is that only *AHA1* is activated by blue light in guard cells. However, the available evidence suggests this is not the case because blue light can elicit H⁺ pumping and induce phosphorylation of H⁺-ATPases in guard cells of *aha1* mutants, although the magnitudes of these responses are small (Fig. 2). We suggest that since the level of *AHA1* protein is greater than those of other isoforms in guard cells, then mutation of *AHA1* greatly decreases the total amount of H⁺-ATPases. This proposal is consistent with our observation of a greatly reduced level of H⁺-ATPase in both *aha1-9* and *aha1-10* mutants (Fig. 2E; Supplemental Fig. S3D), although not in the *aha2* and *aha5* mutants (Fig. 6F). In agreement with these results, a proteomics analysis indicated that only *AHA1* and *AHA9* isoforms are found in guard cell protoplasts (Zhao et al., 2008).

The mutation of *AHA1* in *aha1-10* resulted in a Gly-to-Asp substitution at position 602, which is in the P domain of H⁺-ATPase of Arabidopsis (Fig. 4). This amino acid is highly conserved in the H⁺-ATPase isoforms of both Arabidopsis and other plant species (Supplemental Fig. S9). The mutation in *aha1-10* might produce an aberrant H⁺-ATPase structure, such as a misfolded protein, which is likely degraded in the proteasome pathway (Fig. 7).

We showed that the *AHA1* protein was the most abundant of all *AHA* isoforms in guard cell protoplasts and expected this to be reflected at the mRNA level. However, the transcript level of *AHA1* was the lowest among *AHA1*, *AHA2*, and *AHA5* in protoplasts from wild-type plants (Supplemental Fig. S6). Such discrepancy between the amounts of transcript and protein was also reported in *AHA2* in leaf tissues, in which *AHA2* protein was present although *AHA2* transcript was not detected (Alsterford et al., 2004). Our results accord with a recent transcriptome analysis, which indicated that the transcripts of *AHA5* were higher than those of *AHA1* in intact guard cells (Bauer et al., 2013). Other work reported that the transcripts of *AHA1*, *AHA2*, and *AHA5* were equally expressed in guard cells (Bates et al., 2012). Growth conditions and age of the plants might affect the amount of the H⁺-ATPase proteins present; seasonal changes have been demonstrated to affect pump activity by H⁺-ATPase in guard cells (Lohse and Hedrich, 1992). The presence of a large amount of *AHA1* proteins in guard cells might be regulated by posttranscriptional processes; further investigation will be necessary to determine the cause of this effect.

The mechanisms of red light-induced stomatal opening in plants are a matter of debate. It has been suggested that the opening is mediated by reduction in intercellular CO₂ concentration via photosynthesis in mesophyll chloroplasts and/or action of unidentified substances derived from mesophyll cells (Roelfsema et al., 2006; Lawson et al., 2008; Fujita et al., 2013; Mott et al., 2014), by the action of products generated by guard cell chloroplasts (Schwartz and Zeiger, 1984; Doi and Shimazaki, 2008; Suetsugu et al., 2014), or by

membrane hyperpolarization of guard cells (Serrano et al., 1988). Our results indicate that red light-induced stomatal opening in the *AHA1* mutants *aha1-10* and *aha1-9* was decreased in rate but was not in magnitude. These results imply that the reduced activity of H⁺-ATPase in mutant guard cells was related to the decreased rate of opening. Since H⁺-ATPase maintains the highly hyperpolarized state of guard cells by a steady-state current (Taylor and Assmann, 2001; Roelfsema et al., 2002), the reduction of the H⁺-ATPase activity might result a higher likeliness of guard cells to shift to a more depolarized state in the mutant, in comparison to the wild type. The hyperpolarized membrane potential supports the high turgor pressure in guard cells and is likely to be in a prepared state for opening stomata quickly in response to red light. Red light may reduce the CO₂ concentration and cause the inactivation of anion channels; the basal current of H⁺-ATPase in guard cells may favor stomatal opening in collaboration with the inactivation of anion channels. Further investigations will be needed to clarify this mechanism.

MATERIALS AND METHODS

Plant Materials and Growth Conditions

Arabidopsis (*Arabidopsis thaliana*) ecotypes Col-0 and Col-*g11* were used in all experiments as wild-type plants. M2 seeds from ethyl methanesulfonate-mutagenized plants were obtained from the Nisshoku Group. The *phot1-5 phot2-1* double mutant plant was used as a control showing nonresponsiveness to blue light (Kinoshita et al., 2001). *aha1-9* (*At2g18960*: SAIL_1285_D12), *aha2-4* (*At4g30190*: SALK_082786; Haruta et al., 2010), and *aha5-2* (*At2g24520*: SALK_010589) were obtained from the Nottingham Arabidopsis Stock Center (NASC). The Col-*g11* background *ost2-3D* mutant was previously isolated in a mutant screen using infrared thermography (Takemiya et al., 2013b). For mutant screening, the mutagenized plants were grown in 0.8% agarose plates containing 2.3 mM MES-NaOH (pH 5.7), 1% (w/v) Suc, and half-strength Murashige-Skoog salts for 10 d under continuous white light (60 $\mu\text{mol m}^{-2} \text{s}^{-1}$) at 23°C. The plants were then transferred to 1:1 soil and vermiculite mixture and grown for 8 d under white light (60 $\mu\text{mol m}^{-2} \text{s}^{-1}$) with 13-h/11-h light/dark cycle. The plants used for other experiments were grown in 1:1 soil and vermiculite mixture for 4 weeks under white light (60 $\mu\text{mol m}^{-2} \text{s}^{-1}$) with 14-h/10-h light/dark cycle.

Determination of Changes in Leaf Temperature by Infrared Thermography

Leaf temperature was determined by infrared thermography as previously described (Takemiya et al., 2013b). Briefly, plants were kept in the dark at 21 to 24°C and 40 to 50% relative humidity and illuminated with red light (80 $\mu\text{mol m}^{-2} \text{s}^{-1}$) for 50 min, and then a continuous weak blue light (5 $\mu\text{mol m}^{-2} \text{s}^{-1}$) was superimposed on the red light. The temperature decrease was visualized by subtraction of thermal images created before and after 15 min illumination with blue light using PE Professional software (NEC Avio Infrared Technologies).

Stomatal Aperture and Gas Exchange

The dark-adapted epidermal peels were floated on 1 mL of basal reaction mixture and illuminated with red light (60 $\mu\text{mol m}^{-2} \text{s}^{-1}$) or red light (50 $\mu\text{mol m}^{-2} \text{s}^{-1}$) and blue light (10 $\mu\text{mol m}^{-2} \text{s}^{-1}$) or treated with fusicoccin at 10 μM in the dark for 2 h. Basal reaction mixtures contained 5 mM MES-BTP (Bis-Tris propane), pH 6.5, 50 mM KCl, and 0.1 mM CaCl₂. Stomatal apertures of abaxial epidermis were measured using a microscope (Eclipse TS100; Nikon).

Stomatal conductance was determined using a portable gas exchange system (Li6400; Li-Cor) equipped with an Arabidopsis leaf chamber (6400-15; Li-Cor). The measurements were performed with an airflow of 200 L h⁻¹, 350 ppm CO₂, relative humidity of 40 to 60%, and 24°C. The leaf was illuminated with red light

(600 $\mu\text{mol m}^{-2} \text{s}^{-1}$) for 50 min and then with superimposed blue light (20 $\mu\text{mol m}^{-2} \text{s}^{-1}$) for 20 min. Data were recorded at 10-s intervals.

Isolation of Guard Cell Protoplasts

Guard cell protoplasts were isolated enzymatically from 4- to 5-week-old leaves of Arabidopsis as described previously (Ueno et al., 2005; Takemiya et al., 2013b). The typical yield of guard cell protoplasts was 4.3×10^7 cells per 5,000 leaves with a purity of 98%.

Blue Light- and Fusicoccin-Dependent H⁺ Pumping

Blue light- and fusicoccin-dependent H⁺ pumping was determined using a glass pH electrode as described previously (Ueno et al., 2005). The reaction mixture (0.8 mL) contained 0.125 mM MES-NaOH (pH 6.0), 1 mM CaCl₂, 10 mM KCl, 0.4 M mannitol, and 50 μg proteins.

Effect of Protease Inhibitors on the Amount of H⁺-ATPase

Guard cell protoplasts were treated with 26S proteasome inhibitors MG132 (50 μM ; Sigma-Aldrich) and Ser protease inhibitor apronitin (10 μM ; Calbiochem) with 2 mM DTT (Nacalai Tesque), 1 mM N^α-tosyl-lys chloromethyl ketone (TLCK; Calbiochem), and 1% protease inhibitor cocktail Set III (Calbiochem) by incubation of the protoplasts with each chemical for 30 min at 24°C. Guard cell protoplasts were also treated with 5 mM PMSF (Nacalai Tesque) for 30 min at 24°C in the same manner. The reaction suspensions contained 0.125 mM MES-NaOH (pH 6.0), 1 mM CaCl₂, 10 mM KCl, 0.4 M mannitol, 1% DMSO, and 5 μg proteins from guard cell protoplasts. Reactions were stopped with trichloroacetic acid (Nacalai Tesque) at the indicated times. The mixtures were kept on ice for 10 min followed by centrifugation for 10 min at 14,000 rpm, 4°C. The pellets were washed with 50 mM Tris-HCl (pH 8.0) and used for SDS-PAGE.

Analyses of Protein Blots and Immunoblots

Guard cell protoplasts were incubated in a reaction mixture (0.7 mL) containing 0.125 mM MES-NaOH (pH 6.0), 1 mM CaCl₂, 10 mM KCl, and 0.4 M mannitol. Guard cell protoplasts were illuminated with red light (60 $\mu\text{mol m}^{-2} \text{s}^{-1}$) for 30 min and then a pulse of blue light (100 $\mu\text{mol m}^{-2} \text{s}^{-1}$) was applied for 30 s. Phosphorylation of the penultimate Thr in H⁺-ATPase was determined by a protein blot using GST-14-3-3 ϕ with slight modifications of the described method (Kinoshita and Shimazaki, 1999; Sennelid et al., 1999). The amount of H⁺-ATPase was determined by immunoblotting (Takemiya et al., 2013a). *phot1*, *phot2*, and BLUS1 were identified by immunodetection with polyclonal antibodies as described (Kinoshita et al., 2001; Takemiya et al., 2013b). Phosphorylation of BLUS1 at Ser-348 was determined by antibodies that recognize blue light-specific phosphorylation in BLUS1 (Takemiya et al., 2013b).

Resequencing and Detection of Single-Nucleotide Polymorphisms

Genomic DNAs from Col-*g11*, F2 population of back crossed with *blus2*, and Landsberg *erecta*, were extracted with Plant DNeasy mini kit (Qiagen). Libraries were prepared using NEBNext DNA Library Prep Reagent Set for Illumina (NEB) after sonication with Covaris S2. For adaptors and primers, NEB Next Singleplex Oligos for Illumina were used. Sequencing was conducted on a GAIIx (Illumina). Sequence data were imported into Strand NGS software (Agilent), and alignment of 75-nucleotide reads to reference Arabidopsis Col-0 genome was performed using the COBweb algorithm using the following parameters: minimum alignment score, 95; number of gaps allowed, 5; number of matches to be output for each read, 1; ignore reads with alignment length <25; trim 3' end with average base quality less than 10. After filtering the mapped read with Tile Quality filter in Strand NGS, Bayesian-based single-nucleotide polymorphisms were extracted in Strand NGS using the following parameters: ignore reference locations with coverage below 10; ignore reference locations with variants below 6; confidence score cutoff, 30. Effects by single-nucleotide polymorphisms were detected on annotated genes and then further analyzed with Microsoft Excel. Raw sequence data were deposited in DDBJ Sequence Read Archive (DNA Data Bank of Japan: accession number DRA003952). The analyses of *blus2* and other mutants were carried out simultaneously. Reads of the other mutants will be published elsewhere.

Vector Construction and Generation of Transgenic Plants

We constructed the *AHA1* genomic region $-4,188$ bp to $+6,843$ bp from the start ATG. The 5,106-bp region from $-4,188$ bp to $+918$ bp was amplified using the following primers: 5'-GGCCAGTCCCAAGCTTCTACTACACATACATGATGC-3' and 5'-GTAGCAATCAGAATTCACAAGTTGCTTCTACTGATAG-3'. The product was purified and ligated into pRI101-AN (Takara), digested with *Hind*III and *Eco*RI using the infusion HD cloning kit (Clontech). The 5,602-bp region including $+918$ bp to $+6,843$ bp was amplified using the following primers: 5'-AGCAACTTGTGAATTCCTCTATTGTAATTGATTTG-3' and 5-GTAGCAATCAGAATTCATCCATATCTTTGGACGTG-3'. The product was purified and ligated into the vector with a genomic fragment cut with *Eco*RI using the infusion HD cloning kit. The construct was transformed into *blus2* using *Agrobacterium tumefaciens*-mediated transformation.

RT-PCR and Real-Time PCR Analysis

Total RNAs were extracted from leaves and guard cell protoplasts using RNeasy (Qiagen). First-strand cDNA was synthesized from 500 ng of total RNA using the Superscript III First-strand Synthesis System (Invitrogen). The primer sets for RT-PCR were 5'-GGAATTCATGTTCAGGTCTCGAAGATATCAA-GAACG-3' and 5'-CGGGATCCCTACACAGTGTAGTGTGCTG-3' for *AHA1*; 5'-GGAATTCATGTTCAGTCTCGAAGATATCAAAGAACG-3' and 5'-CGGGATCCCTACACAGTGTAGTGTGCTG-3' for *AHA2*; 5'-GGAATTCATGTTCAGTGTTCGAGGAGC-3' and 5'-CGGGATCCCTAAACGGTGTAAATGTGCTGAATCGTG-3' for *AHA5*; and 5'-ACTTACGCCAGTGGTCTGACAC-3' and 5'-AAGGACTTCTGGCACCTGAATCT-3' for *ACT8*.

Real-time PCR was performed using the Brilliant III Ultra-Fast SYBR Green QPCR Master Mix (Agilent) and MxP3000 QPCR system (Stratagene). The primer sets for gene specific amplification were 5'-GCTATGGCTTCTAGGGTGG-3' and 5'-GCCAGTACCATCAGAGTCCG-3' for *AHA1*; 5'-TGAACGTCCTGGAGCA-TTG-3' and 5'-TTCCAGTTGGCTAAACC-3' for *AHA2*; and 5'-GAAGAAA-GATGCTCCTGGT-3' and 5'-CCTGATTGCTCGGCACTGT-3' for *AHA5*. The *AHA2* primers were described previously (Haruta et al., 2010). A standard linear curve for absolute quantification was created using pBluescript II KS+ (Stratagene) containing *AHA1*, *AHA2*, or *AHA5* CDS with serial dilution from 0 to 10^5 copies.

Preparation and Immunodetection of GST Fusion Protein

The catalytic regions of *AHA1*, *AHA2*, and *AHA5* from cDNA were subcloned into the pGEX-2T vector (Pharmacia Biotech) and introduced into *Escherichia coli* strain Rosetta-gami B (Merck) using the following primer sets: 5'-TGTTCCCGCTAGGTTGTCTGTGACTATGGCTATC-3' and 5'-GATG-AATCCCGCTAGAAATCCCATATCAAAGCAATAAGC-3' for *AHA1*; 5'-TGTTCCCGCTAGGTTGTCTGTGACTATGGCTATC-3' and 5'-GATG-AATCCCGCTAGAAATCCCATATCAAAGCAATAAGC-3' for *AHA2*; and 5'-TGTTCCCGCTAGGTTGTCTGTGACTATGGCTATC-3' and 5'-GATG-AATCCCGCTAGGTTGTCTGTGACTATGGCTATC-3' for *AHA5*.

E. coli cells were grown as described previously with slight modification (Takemiya et al., 2013a). GST-AHAs were purified using glutathione-sepharose (GE Healthcare). Recombinant proteins were detected by immunoblotting using anti- H^+ -ATPase antibodies (Kinoshita and Shimazaki, 1999).

Statistical Analysis

Significant differences were identified using Student *t* tests. Student *t* tests were performed using Microsoft Excel. Two-sided tests were carried out for homoscedastic matrices.

Accession Numbers

Sequence data from this article can be found in the DNA Data Bank of Japan Sequence Read Archive under accession number DRA003952.

Supplemental Data

The following supplemental materials are available.

Supplemental Figure S1. Reverse transcription-PCR analysis of *AHA1* in guard cells of *blus2*.

Supplemental Figure S2. Identification of *aha1-9* allele.

Supplemental Figure S3. *aha1-9* allele phenotype in guard cells.

Supplemental Figure S4. Genetic analysis of *blus2* and *aha1-9*.

Supplemental Figure S5. Identification and analyses of *aha2-4* and *aha5-2*.

Supplemental Figure S6. Immunoblot analysis of recombinant *AHA1*, *AHA2*, and *AHA5*.

Supplemental Figure S7. Absolute quantification of *AHA1*, *AHA2*, and *AHA5* by real-time PCR.

Supplemental Figure S8. Effects of protease inhibitors on the amount of H^+ -ATPase in guard cell protoplasts.

Supplemental Figure S9. Amino acid sequence alignment of H^+ -ATPase isoforms and orthologs.

ACKNOWLEDGMENTS

We thank Dr. T. Matsushita (Kyushu University) for valuable suggestions regarding mutant screening and mutant analyses and F. Oba and M. Aibe for their helpful technical assistance. We also thank the Salk Institute Genomic Analysis Laboratory for providing the sequence indexed Arabidopsis T-DNA insertion mutants and the NASC for providing the seeds used in this work.

Received April 5, 2016; accepted June 2, 2016; published June 3, 2016.

LITERATURE CITED

- Alsterfjord M, Sehnke PC, Arkell A, Larsson H, Svennelid F, Rosenquist M, Ferl RJ, Sommarin M, Larsson C (2004) Plasma membrane H^+ -ATPase and 14-3-3 isoforms of Arabidopsis leaves: evidence for isoform specificity in the 14-3-3/ H^+ -ATPase interaction. *Plant Cell Physiol* **45**: 1202–1210
- Arango M, Gévaudant F, Oufattole M, Boutry M (2003) The plasma membrane proton pump ATPase: the significance of gene subfamilies. *Planta* **216**: 355–365
- Assmann SM (1993) Signal transduction in guard cells. *Annu Rev Cell Biol* **9**: 345–375
- Bates GW, Rosenthal DM, Sun J, Chattopadhyay M, Peffer E, Yang J, Ort DR, Jones AM (2012) A comparative study of the *Arabidopsis thaliana* guard-cell transcriptome and its modulation by sucrose. *PLoS One* **7**: e49641
- Bauer H, Ache P, Lautner S, Fromm J, Hartung W, Al-Rasheid KA, Sonnewald S, Sonnewald U, Kneitz S, Lachmann N, et al (2013) The stomatal response to reduced relative humidity requires guard cell-autonomous ABA synthesis. *Curr Biol* **23**: 53–57
- Baxter IR, Young JC, Armstrong G, Foster N, Bogenschütz N, Cordova T, Peer WA, Hazen SP, Murphy AS, Harper JF (2005) A plasma membrane H^+ -ATPase is required for the formation of proanthocyanidins in the seed coat endothelium of *Arabidopsis thaliana*. *Proc Natl Acad Sci USA* **102**: 2649–2654
- Briggs WR, Christie JM (2002) Phototropins 1 and 2: versatile plant blue-light receptors. *Trends Plant Sci* **7**: 204–210
- Christie JM (2007) Phototropin blue-light receptors. *Annu Rev Plant Biol* **58**: 21–45
- Doi M, Kitagawa Y, Shimazaki K (2015) Stomatal blue light response is present in early vascular plants. *Plant Physiol* **169**: 1205–1213
- Doi M, Shimazaki K (2008) The stomata of the fern *Adiantum capillus-veneris* do not respond to CO_2 in the dark and open by photosynthesis in guard cells. *Plant Physiol* **147**: 922–930
- Doi M, Wada M, Shimazaki K (2006) The fern *Adiantum capillus-veneris* lacks stomatal responses to blue light. *Plant Cell Physiol* **47**: 748–755
- Fujita T, Noguchi K, Terashima I (2013) Apoplastic mesophyll signals induce rapid stomatal responses to CO_2 in *Commelina communis*. *New Phytol* **199**: 395–406
- Haruta M, Burch HL, Nelson RB, Barrett-Wilt G, Kline KG, Mohsin SB, Young JC, Otegui MS, Sussman MR (2010) Molecular characterization of mutant Arabidopsis plants with reduced plasma membrane proton pump activity. *J Biol Chem* **285**: 17918–17929
- Hetherington AM, Woodward FI (2003) The role of stomata in sensing and driving environmental change. *Nature* **424**: 901–908
- Inoue S, Kinoshita T, Matsumoto M, Nakayama KI, Doi M, Shimazaki K (2008) Blue light-induced autophosphorylation of phototropin is a primary step for signaling. *Proc Natl Acad Sci USA* **105**: 5626–5631

- Inoue S, Matsushita T, Tomokiyo Y, Matsumoto M, Nakayama KI, Kinoshita T, Shimazaki K (2011) Functional analyses of the activation loop of phototropin2 in *Arabidopsis*. *Plant Physiol* **156**: 117–128
- Inoue S, Takemiya A, Shimazaki K (2010) Phototropin signaling and stomatal opening as a model case. *Curr Opin Plant Biol* **13**: 587–593
- Kerkeb L, Venema K, Donaire JP, Rodríguez-Rosales MP (2002) Enhanced H⁺/ATP coupling ratio of H⁺-ATPase and increased 14-3-3 protein content in plasma membrane of tomato cells upon osmotic shock. *Physiol Plant* **116**: 37–41
- Kim TH, Böhmer M, Hu H, Nishimura N, Schroeder JI (2010) Guard cell signal transduction network: advances in understanding abscisic acid, CO₂, and Ca²⁺ signaling. *Annu Rev Plant Biol* **61**: 561–591
- Kinoshita T, Doi M, Suetsugu N, Kagawa T, Wada M, Shimazaki K (2001) Phot1 and phot2 mediate blue light regulation of stomatal opening. *Nature* **414**: 656–660
- Kinoshita T, Shimazaki K (1999) Blue light activates the plasma membrane H⁺-ATPase by phosphorylation of the C-terminus in stomatal guard cells. *EMBO J* **18**: 5548–5558
- Lawson T, Lefebvre S, Baker NR, Morison JIL, Raines CA (2008) Reductions in mesophyll and guard cell photosynthesis impact on the control of stomatal responses to light and CO₂. *J Exp Bot* **59**: 3609–3619
- Lorenzo ME, Jung JU, Ploegh HL (2002) Kaposi's sarcoma-associated herpesvirus K3 utilizes the ubiquitin-proteasome system in routing class major histocompatibility complexes to late endocytic compartments. *J Virol* **76**: 5522–5531
- Lohse G, Hedrich R (1992) Characterization of the plasma-membrane H⁺-ATPase from *Vicia faba* guard cells: Modulation by extracellular factors and seasonal changes. *Planta* **188**: 206–214
- Marten H, Hedrich R, Roelfsema MRG (2007) Blue light inhibits guard cell plasma membrane anion channels in a phototropin-dependent manner. *Plant J* **50**: 29–39
- Merlot S, Leonhardt N, Fenzi F, Valon C, Costa M, Piette L, Vavasseur A, Genty B, Boivin K, Müller A, Giraudat J, Leung J (2007) Constitutive activation of a plasma membrane H⁺-ATPase prevents abscisic acid-mediated stomatal closure. *EMBO J* **26**: 3216–3226
- Mott KA, Berg DG, Hunt SM, Peak D (2014) Is the signal from the mesophyll to the guard cells a vapour-phase ion? *Plant Cell Environ* **37**: 1184–1191
- Negi J, Matsuda O, Nagasawa T, Oba Y, Takahashi H, Kawai-Yamada M, Uchimiya H, Hashimoto M, Iba K (2008) CO₂ regulator SLAC1 and its homologues are essential for anion homeostasis in plant cells. *Nature* **452**: 483–486
- Niittylä T, Fuglsang AT, Palmgren MG, Frommer WB, Schulze WX (2007) Temporal analysis of sucrose-induced phosphorylation changes in plasma membrane proteins of *Arabidopsis*. *Mol Cell Proteomics* **6**: 1711–1726
- Okumura M, Inoue S, Kuwata K, Kinoshita T (2016) Photosynthesis activates plasma membrane H⁺-ATPase via sugar accumulation. *Plant Physiol* **171**: 580–589
- Pandey S, Zhang W, Assmann SM (2007) Roles of ion channels and transporters in guard cell signal transduction. *FEBS Lett* **581**: 2325–2336
- Palmgren MG (2001) PLANT PLASMA MEMBRANE H⁺-ATPASE: powerhouses for nutrient uptake. *Annu Rev Plant Physiol* **52**: 817–845
- Piper RC, Luzio JP (2007) Ubiquitin-dependent sorting of integral membrane proteins for degradation in lysosomes. *Curr Opin Cell Biol* **19**: 459–465
- Robertson WR, Clark K, Young JC, Sussman MR (2004) An *Arabidopsis thaliana* plasma membrane proton pump is essential for pollen development. *Genetics* **168**: 1677–1687
- Roelfsema MRG, Hanstein S, Felle HH, Hedrich R (2002) CO₂ provides an intermediate link in the red light response of guard cells. *Plant J* **32**: 65–75
- Roelfsema MRG, Hedrich R (2005) In the light of stomatal opening: new insights into 'the Watergate'. *New Phytol* **167**: 665–691
- Roelfsema MRG, Konrad KR, Marten H, Psaras GK, Hartung W, Hedrich R (2006) Guard cells in albino leaf patches do not respond to photosynthetically active radiation, but are sensitive to blue light, CO₂ and abscisic acid. *Plant Cell Environ* **29**: 1595–1605
- Schmitz A, Herzog V (2004) Endoplasmic reticulum-associated degradation: exceptions to the rule. *Eur J Cell Biol* **83**: 501–509
- Schwartz A, Zeiger E (1984) Metabolic energy for stomatal opening. Roles of photophosphorylation and oxidative phosphorylation. *Planta* **161**: 129–136
- Serrano EE, Zeiger E, Hagiwara S (1988) Red light stimulates an electrogenic proton pump in *Vicia* guard cell protoplasts. *Proc Natl Acad Sci USA* **85**: 436–440
- Shimazaki K, Doi M, Assmann SM, Kinoshita T (2007) Light regulation of stomatal movement. *Annu Rev Plant Biol* **58**: 219–247
- Suetsugu N, Takami T, Ebisu Y, Watanabe H, Iiboshi C, Doi M, Shimazaki K (2014) Guard cell chloroplasts are essential for blue light-dependent stomatal opening in *Arabidopsis*. *PLoS One* **9**: e108374
- Svennelid F, Olsson A, Piotrowski M, Rosenquist M, Ottman C, Larsson C, Oecking C, Sommarin M (1999) Phosphorylation of Thr-948 at the C terminus of the plasma membrane H⁺-ATPase creates a binding site for the regulatory 14-3-3 protein. *Plant Cell* **11**: 2379–2391
- Takahashi K, Hayashi K, Kinoshita T (2012) Auxin activates the plasma membrane H⁺-ATPase by phosphorylation during hypocotyl elongation in *Arabidopsis*. *Plant Physiol* **159**: 632–641
- Takemiya A, Kinoshita T, Asanuma M, Shimazaki K (2006) Protein phosphatase 1 positively regulates stomatal opening in response to blue light in *Vicia faba*. *Proc Natl Acad Sci USA* **103**: 13549–13554
- Takemiya A, Yamauchi S, Yano T, Ariyoshi C, Shimazaki K (2013a) Identification of a regulatory subunit of protein phosphatase 1 which mediates blue light signaling for stomatal opening. *Plant Cell Physiol* **54**: 24–35
- Takemiya A, Sugiyama N, Fujimoto H, Tsutsumi T, Yamauchi S, Hiyama A, Tada Y, Christie JM, Shimazaki K (2013b) Phosphorylation of BLUS1 kinase by phototropins is a primary step in stomatal opening. *Nat Commun* **4**: 2094
- Taylor AR, Assmann SM (2001) Apparent absence of a redox requirement for blue light activation of pump current in broad bean guard cells. *Plant Physiol* **125**: 329–338
- Tokutomi S, Matsuoka D, Zikihara K (2008) Molecular structure and regulation of phototropin kinase by blue light. *Biochim Biophys Acta* **1784**: 133–142
- Ueno K, Kinoshita T, Inoue S, Emi T, Shimazaki K (2005) Biochemical characterization of plasma membrane H⁺-ATPase activation in guard cell protoplasts of *Arabidopsis thaliana* in response to blue light. *Plant Cell Physiol* **46**: 955–963
- Vahisalu T, Kollist H, Wang YF, Nishimura N, Chan WY, Valerio G, Lamminmäki A, Brosché M, Moldau H, Desikan R, Schroeder JI, Kangasjärvi J (2008) SLAC1 is required for plant guard cell S-type anion channel function in stomatal signalling. *Nature* **452**: 487–491
- Vavasseur A, Raghavendra AS (2005) Guard cell metabolism and CO₂ sensing. *New Phytol* **165**: 665–682
- Vitart V, Baxter I, Doerner P, Harper JF (2001) Evidence for a role in growth and salt resistance of a plasma membrane H⁺-ATPase in the root endodermis. *Plant J* **27**: 191–201
- Wang Y, Noguchi K, Ono N, Inoue S, Terashima I, Kinoshita T (2014) Overexpression of plasma membrane H⁺-ATPase in guard cells promotes light-induced stomatal opening and enhances plant growth. *Proc Natl Acad Sci USA* **111**: 533–538
- Zhao X, Qiao XR, Yuan J, Ma XF, Zhang X (2012) Nitric oxide inhibits blue light-induced stomatal opening by regulating the K⁺ influx in guard cells. *Plant Sci* **184**: 29–35
- Zhao Z, Zhang W, Stanley BA, Assmann SM (2008) Functional proteomics of *Arabidopsis thaliana* guard cells uncovers new stomatal signaling pathways. *Plant Cell* **20**: 3210–3226